© 2020. Published by The Company of Biologists Ltd | Journal of Experimental Biology (2020) 223, jeb219808. doi:10.1242/jeb.219808

RESEARCH ARTICLE

A mechanical approach to understanding the impact of the nematode *Anguillicoloides crassus* on the European eel swimbladder

Helen A. L. Currie*, Nicholas Flores Martin, Gerardo Espindola Garcia, Frances M. Davis and Paul S. Kemp

ABSTRACT

One of the most detrimental factors in the drastic decline of the critically endangered European eel (*Anguilla anguilla*) was the inadvertent introduction of the invasive nematode *Anguillicoloides crassus*. Infection primarily affects the swimbladder, a gas-filled organ that enables the eel to control its depth in the water. A reduction in swimbladder function may be fatal for eel undergoing their spawning migration to the Sargasso Sea, a journey of over 5000 km. Although the physiological damage caused by this invasive parasite is well studied through the use of quantifiable gross pathological indices, providing a good measure of the swimbladder health status, they cannot separate the role of mechanical and morphological damage. Our study examined the appropriateness of three commonly used indices as a measure of mechanical damage by performing uniaxial tensile tests on swimbladder specimens obtained from an infected eel population. When the test results were compared with the gross pathological indices it was found that thickness correlated most strongly with mechanical damage, both confirming and, more importantly, explaining the counterintuitive findings of earlier work. In a damaged swimbladder, the immune response leads to a trade-off; increasing wall thickness raises the pressure required for organ rupture but decreases strength. The results indicate that for moderate infection the mechanical integrity of the swimbladder can be maintained. For severe infection, however, a reduction in mechanical integrity may reach a tipping point, thereby affecting the successful completion of their oceanic migration.

KEY WORDS: European eel, Mechanical damage, Parasite, Swimbladder

INTRODUCTION

Over the last 40 years, drastic declines in the European eel (*Anguilla anguilla*) population have been observed throughout Europe, with reductions in adult silver eel escapement of 50–60% (Aalto et al., 2016; ICES, 2017), and 90–95% in juvenile glass eel recruitment (Bornarel et al., 2018; Dekker, 2003; ICES, 2017). The European eel is listed as 'critically endangered' [International Union for Conservation of Nature (IUCN) Red List] and stocks are considered to be outside safe biological limits (Jacoby and Gollock, 2014). Numerous factors have been identified to explain the decline, including shifts in oceanographic conditions (Baltazar-Soares et al., 2014), over-exploitation (Jacoby et al., 2015), anthropogenic barriers to migration and habitat loss (Acou et al., 2008; Jacoby et al., 2015; Miller et al., 2015), disease (Jacoby et al., 2015) and parasite infection (Kirk, 2003).

Arguably, one of the most detrimental factors contributing to population decline is the introduction of the invasive parasite, *Anguillicoloides crassus* (Barry et al., 2014; Lefebvre et al., 2002; Palstra et al., 2007). Inadvertently introduced in the late 1980s via imports for aquaculture of its native host, the Japanese eel (*Anguilla japonica*), *A. crassus* spread quickly and became highly prevalent across Europe (Kennedy, 1993; Wielgoss et al., 2008). The swimbladder-residing nematode causes structural and inflammatory pathological damage within the naïve European eel (Lefebvre et al., 2012; Molnár et al., 1993), and has the capacity to exceed 90% prevalence over a 4-year period of establishment (Knopf, 2006; Lefebvre et al., 2013). The resulting immune responses lead to a reduced swimbladder volume and thickening of its walls (Beregi et al., 1998; Molnár et al., 1993; Nimeth et al., 2000). The host is liable to reinfection across a range of life stages (see Fig. S1 for a description of the *A. crassus* life cycle) and, owing to a relatively short generation time in comparison with its host (De Charleroy et al., 1990), the presence or absence of nematodes provides little to no information on infection history (Lefebvre et al., 2013).

Anguillicoloides crassus infection affects the overall functioning of the swimbladder, potentially affecting buoyancy control. During the early stages of their oceanic migration to the Sargasso Sea, a distance of approximately 5000–6000 km, adult silver eel exhibit diel vertical migrations during which they reach depths that range between 200 and 1000 m (Aarestrup et al., 2009; Righton et al., 2016). This equates to a difference in hydrostatic pressure of up to 8 MPa. Damage to the swimbladder could reduce fitness by increasing the energetic costs required to swim during migration (Newbold et al., 2015; Palstra et al., 2007; van den Thillart et al., 2004), for example by hindering metabolic processes reliant on gas gland cell activity (Pelster, 2015), or inhibiting the ability to effectively regulate body position within the water column (Palstra et al., 2007). Furthermore, it is hypothesised that if an individual does not enter deeper oceanic waters, the process of sexual maturation cannot be completed (Sébert et al., 2007; Sjöberg et al., 2009). High hydrostatic pressure triggers an increase in pituitary–gonad axis activity, raising plasma levels of sex steroids (Sébert et al., 2007; Sjöberg et al., 2009). It is suggested that any reduction in organ control may threaten successful completion of transoceanic migrations, spawning activity and subsequent next generation recruitment (Lefebvre et al., 2013; Székely et al., 2009).

Several retrospective studies have been performed on the European eel to grade the degree of swimbladder deterioration

International Centre for Ecohydraulics Research, Faculty of Engineering and Physical Sciences, Boldrewood Innovation Campus, University of Southampton, Southampton SO16 7QF, UK.

*Author for correspondence (Helen.Currie@soton.ac.uk)

H.A.L.C., 0000-0001-5792-3488; P.S.K., 0000-0003-4470-0589

Received 5 December 2019; Accepted 30 June 2020

Journal of Experimental Biology (2020) 223, jeb219808. doi:10.1242/jeb.219808

caused by *A. crassus* and, as a result, numerous damage indices have been developed. The three most common indices used in the literature are wall thickness (Molnár et al., 1993), parasite load (Lefebvre et al., 2002) and length ratio index (LRI) (Lefebvre et al., 2011; Palstra et al., 2007). Each of these indices rely on observation of the gross pathology of the swimbladder after autopsy, with the latter calculated by dividing the length of the swimbladder by the total length of the eel. It has been suggested as a quantifiably appropriate index as swimbladders thicken and shorten as a result of multiple infection events (Lefebvre et al., 2011). Wall thickness and LRI have been shown to track the severity of cumulative infections (Lefebvre et al., 2011; Molnár et al., 1993) and parasite-induced reductions of swimming speed (Palstra et al., 2007), respectively, while parasite load is a common metric used to estimate the current parasite pressure on an eel (Lefebvre et al., 2002). While these measures of damage perform the critical function of assessing the health of the eel swimbladder, they are global measurements that do not directly indicate the mechanisms that lead to degradation of swimbladder function. Barry et al. (2014) were the first to attempt to link the impact of infection to the rupture response of eel swimbladders. They inflated intact swimbladders from infected and uninfected eel and found that the pressure required to rupture infected swimbladders was greater than for those that were uninfected. This result is at odds with histological evidence (Molnár et al., 1993, 1995; Sokolowski and Dove, 2006), which indicates that infected bladders are damaged and exhibit inflammation and hyperplasia. Their study highlights the complexity of performing tests on an entire organ. By testing the entire swimbladder, Barry et al. (2014) performed a structural test in which the outcome depends on both the geometry and mechanical response of each sample. As a result, it remains unclear whether infection and pathological damage degrade the mechanical response of the swimbladder wall. Furthermore, as neither the underlying mechanical properties nor the geometry of the specimen are known, it is difficult to quantify the impact of wall thickening on the rupture pressure.

Damage indices have largely relied on the degree of histopathological damage (Lefebvre et al., 2002, 2011) and measures of overall eel health (Palstra et al., 2007), which necessarily include the impact of *A. crassus* on the mechanical and the biochemical response (gas secretion and diffusion) of the swimbladder wall. This study aims to disentangle the mechanical response from the morphological (structural) changes caused by *A. crassus* by characterising the rupture strength and elasticity of the swimbladder wall at various stages of infection. In part 1 of this study, differences between samples obtained from geographically distinct catchments were tested to ascertain whether different environmental experiences have an impact on parasite infection history, or physiological development and subsequent swimbladder mechanical response. Additionally, the relationship between the mechanical response (rupture strength and elasticity) and morphological damage indices (swimbladder wall thickness, LRI and parasite load) were investigated in part 2 of this study. As most biological materials exhibit anisotropy (direction-dependent mechanical properties) due to the underlying organisation of collagen fibres, these relationships were determined in both the longitudinal and circumferential direction. This interdisciplinary study provides new explanation and insight on the mechanisms that underpin swimbladder response to *A. crassus* infection, a potential contributor to the decline of European eel populations throughout their range.

MATERIALS AND METHODS

Subject species

In line with the principles of the ethical use of animals in research (Russell and Burch, 1959) in which the numbers of animals used should be reduced to the minimum expected to provide statistically robust results, the swimbladders used in this experiment were obtained from eel used in two previous behavioural studies (N_{total1}=174; N_{total2}=85) conducted at the International Centre for Ecohydraulics Research (ICER) (M. Miller, J. de Bie, A. Haro, S. M. Sharkh and P.S.K., unpublished data; A. S. Vowles, P. Vezza, C. Manes and P.S.K., unpublished data). European eel [*Anguilla anguilla* (Linnaeus 1758)] were obtained from the River Test, Hampshire (50°55.714′ N, 01°29.232′ W; N_{tested}=10; length±s.d., 470.5±81.4 mm; wet mass±s.d., 211.1±96.5 g); the River Stour, Dorset (50°46.537′ N, 01°54.644′ W; N_{tested}=10; length, 570.2± 76.87 mm; wet mass, 359.1±155.7 g) and the River Humber, Lincolnshire (53°4.316′ N, 00°12.804′ E; N_{tested}=10; length, 565.7± 34.3 mm; wet mass, 336.9±76.4 g), on 21 November 2016, 2 December 2016 and 26 October 2017, respectively, and captured by commercial fishermen licensed by the Environmental Agency. The eel were transported to the ICER research facilities at the University of Southampton in well-oxygenated transportation tanks, and held in aerated and filtered 3000-litre holding tanks under ambient temperature (mean water temperature±s.d., 10.4±1.9°C). Water quality was checked daily and maintained at optimum levels (NH_3<0.125 p.p.m.; NO_2<0.25 p.p.m.).

Fish were euthanised in accordance with Schedule 1 of the Animals (Scientific Procedures) Act 1986, and the dissection procedure commenced immediately afterwards. The total body length (±1 mm) and wet mass (±0.1 g) of each fish were recorded. Access to the body cavity was via an incision made in the ventral side from the anal opening to the opercula. Gut mass was extracted and swimbladder isolated before being carefully removed together with the ductus pneumaticus. Each swimbladder was measured (to the nearest millimetre) and weighed (±0.01 g). On dissection of the swimbladder, in all cases, nematodes were found detached from the wall enabling ease of removal from the lumen to a Petri dish with minimal use of round-tipped tweezers. The number of nematodes and their total mass (±0.01 g) was recorded. Swimbladder samples were collected for mechanical testing in the circumferential and longitudinal directions (Fig. 1). The width and length of the longitudinal samples were trimmed to approximately 5 mm×15 mm, respectively. While the width of the circumferential samples was cut to approximately 5 mm, due to the variation in size of the swimbladders, the length of circumferential samples varied. Samples were immediately placed in Hanks' Balanced Salt Solution (H6648

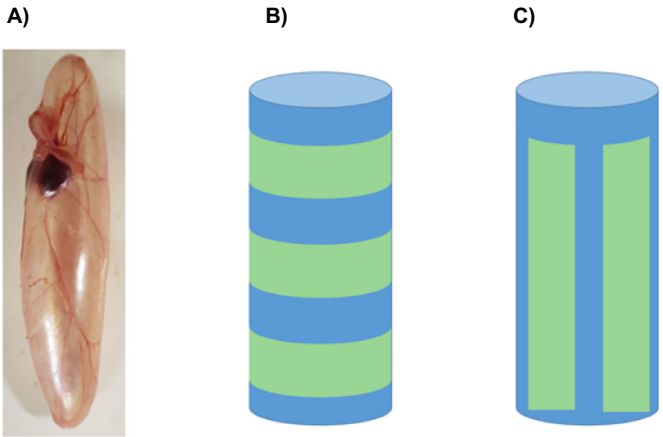

Fig. 1. Swimbladder samples for mechanical testing. (A) European eel swimbladder and schematics showing orientations of the (B) circumferential and (C) longitudinal directions.

9.8 g l^{-1}, Sigma Aldrich, Dorset, UK) and stored at 2°C for up to 36 h prior to mechanical testing.

Ethical note

The study conformed to UK legal requirements (Animals [Scientific Procedures] Act 1986) and was approved by the University of Southampton's Ethics and Research Governance Office (Ethics ID 30580). To adhere to the principles of the 3Rs, the majority of eel obtained for this study were re-utilised from behavioural trials conducted in 2016 and 2017 within ICER (Ethics IDs 23796 and 30639).

Swimbladder morphology and function

The swimbladder wall is composed of four distinct layers: (1) the mucosa, the innermost layer facing the lumen; (2) the muscularis mucosae, a muscle layer; (3) the submucosa, consisting of loose connective tissue; and (4) the serosa, a thin layer with higher cellular density and a matrix of dense connective tissue (Dorn, 1961). A simpler nomenclature has also been suggested, referring to the two internal epithelial layers as the tunica interna, and the outer collagenous layers as the tunica externa (Molnár, et al., 1995). Blood is supplied to the eel swimbladder via the rete mirabile, a bipolar countercurrent system. Gas secretion into the swimbladder is a passive phenomenon that requires a reduction of the physical solubility of gases in the blood by making it more acidic. This is achieved by metabolic activity of the gas gland cells lining the lumen, which produce and secrete lactic acid, subsequently allowing for maintenance of neutral buoyancy (Pelster, 2015). For the purpose of tensile testing, the swimbladder was considered as a single tissue. This approach has previously been used in studies examining the limits of whole swimbladder tissue response to rapid changes in pressure, or 'barotrauma' (e.g. Beirão et al., 2015a,b; Brown et al., 2014).

Mechanical testing

Thirty swimbladders successfully underwent tensile tests. Part 1 of the study compared 10 samples each from the River Stour and River Test, with all samples cut along the longitudinal axis of the swimbladder. Part 2 compared 10 samples cut along the longitudinal axis (River Stour) with 10 cut in the circumferential direction (River Humber) (Fig. 1).

Images of each swimbladder sample were taken using a digital camera (Manta 503B, 2452×2056 px; Allied Vision, Stradtroda, Germany) with a 50 mm lens (Nikkor AF; Nikon, York, United Kingdom). The width of each sample was measured using ImageJ (version 1.51g, National Institutes of Health, Bethesda, MD, USA) where the conversion from pixels to millimetres was determined using a calibration target. Each sample was placed between two plates of known dimensions and the total thickness measured using calipers. The average width and thickness for each sample was determined by taking measurements at a minimum of five locations. The cross-sectional area of each sample was calculated, assuming it to be rectangular, by multiplying the mean width and thickness.

Slippage within the clamps was minimised by wrapping fine grade sandpaper around the end of each sample prior to placing them in the tensile testing device (UStretch; CellScale, Waterloo, Ontario, Canada). A 5 N load cell (LSB200; Futek, Irvine, CA, USA) with a resolution of ±0.02 N was used. Each sample was pre-loaded to 0.05 N and stretched at a speed of 10 mm min^{-1} until failure was visually observed. Load and displacement data were recorded at a frequency of 1 Hz using the UStretch software (version 10.66, CellScale). To determine an accurate failure threshold, the stress (σ; using the first Piola–Kirchoff or engineering stress tensor, where the force is normalised by the initial area) was computed by dividing the current load by the initial cross-sectional area. As a result, the force was normalised by the geometric dimension where the load was applied and was thus comparable between the slightly different-sized samples. Similarly, to account for differences in the sample length, the strain (ε, the Green–Lagrange strain typically calculated in large strain non-linear elasticity), a ratio of extension to original length, was calculated from the initial length (L_0) and the current length (l), which is computed from the displacement data, as follows:

$$\varepsilon = \frac{1}{2}\left(\left(\frac{l}{L_0}\right)^2 - 1\right). \quad (1)$$

To differentiate between the two sample directions, subscript z (e.g. σ_z, ε_z) is used for the longitudinal, and θ (e.g. σ_θ, ε_θ) for the circumferential direction, respectively.

Damage indicators

The relationship between mechanical response of the tissue and the three damage indicators (thickness: Molnár et al., 1993; LRI: Palstra et al., 2007; and parasite load: Lefebvre et al., 2002, 2013) was quantified using criteria for severity of damage (Table 1) based on information available in the literature. The thickness criterion proposed by Molnár et al. (1993) was identified using histology, while Palstra et al. (2007) observed that short swimbladders relative to eel length were frequently highly damaged and reduced swimming endurance. Although these authors reported that the ratio of length of healthy swimbladders to eel length (LRI) is frequently greater than 10%, they did not include any definitive ranges for damaged swimbladders. Notably, the levels for minimal and severe damage are the same for parasite load (Lefebvre et al., 2013); the absence of parasites can indicate both a low or high level of infection as when the swimbladder is severely damaged the parasite can no longer survive in the lumen.

Statistical analysis

Statistical analyses were performed using freeware program RStudio (version 3.2.2, https://rstudio.com/). Two values to measure the differences between the stress–strain curves were calculated: the slope in the linear region and the maximum stress (σ_{max}). The slope was calculated by performing a linear least squares regression in the linear region of the curve (Fig. 2A). The slope provides a measure of the local tangent modulus, which describes how easily a material stretches; higher values indicate greater difficulty (e.g. steel, 205 GPa; silicone rubber, 0.05 GPa). The maximum stress, or rupture strength, is the largest stress value reached before failure. Shapiro–Wilk (normality) and Bartlett's (homoscedasticity) tests were used to determine whether all data met parametric statistical assumptions. Maximum stress and tangent

Table 1. Three commonly used swimbladder damage indicators as a function of estimated parasite infection level

Level of infection	Thickness (mm)[a]	LRI[b]	Parasite load (mg)[c]
None/minimal	$t \leq 0.3$	≥10%	$m_p \leq 3$
Moderate	$0.3 < t \leq 1.5$	<10%	$3 < m_p \leq 20$
Severe	$t \geq 2$		$m_p \leq 3$

t, thickness; LRI, length ratio index; m_p, parasite load (total mass of nematodes). References: [a]Molnár et al. (1993); [b]Palstra et al. (2007); [c]Lefebvre et al. (2013).

Journal of Experimental Biology (2020) 223, jeb219808. doi:10.1242/jeb.219808

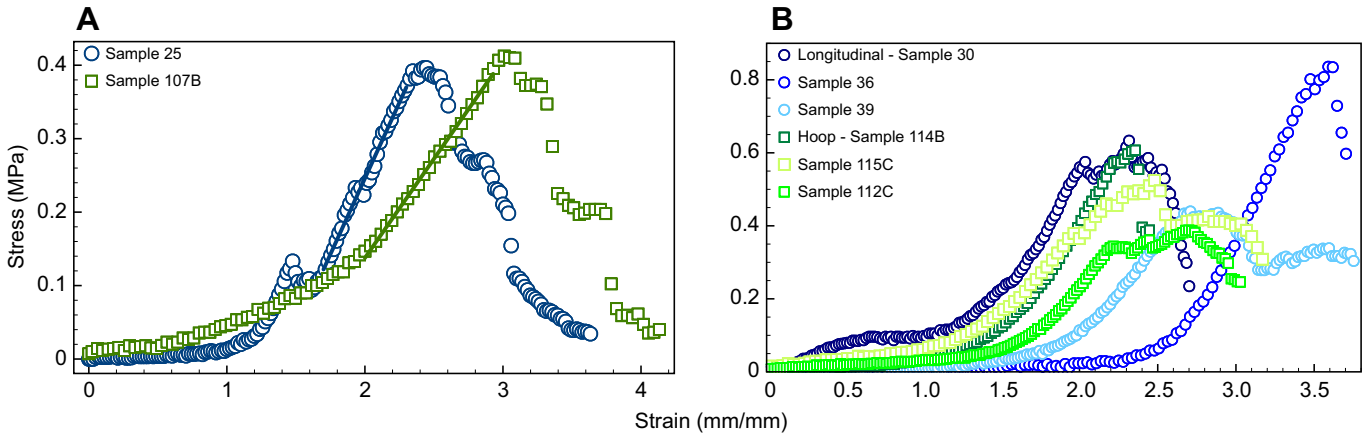

Fig. 2. Non-linear mechanical response of eel swimbladder. (A) Representative fits of the linear region for a stress–strain curve in the longitudinal (circles) and circumferential (squares) direction and (B) resulting stress–strain curves for three swimbladder samples tested in the longitudinal (circles) and circumferential (squares) direction.

modulus data failed to meet assumptive pre-requisites and, therefore, a Mann–Whitney–Wilcoxon test was used to determine if the identified mechanical properties were different between groups of samples. For damage indicators, all three met assumptions of normality; however, parasite load failed to meet assumptions of variance. Therefore, to compare damage indicators in the longitudinal and circumferential direction, thickness and LRI parameters were subject to a Student's *t*-test, and parasite load to Welch's *t*-test. Spearman's rank correlation coefficient was used to determine the relationship between strength and strain between groups for both parts of the experiment, and to identify correlations between mechanical properties and each damage indicator.

RESULTS

Mechanical testing

A total of 20 stress–strain curves in the longitudinal direction and 10 in the circumferential direction were obtained (see Fig. 2 for representative examples). The mechanical responses in both the circumferential and longitudinal direction were non-linear as typically associated with fibrous soft tissues. In part 1 of the study, there was no interpopulation (River Stour and River Test) difference between modulus (t_{20}=0.33, P=0.74) and maximum stress (t_{20}=−1.23, P=0.23) of exclusively longitudinal samples. This result validated the inclusion of fish from differing populations in part 2 of our analysis. Subsequently, in part 2 the mechanical responses differed with directionality (circumferential versus longitudinal).

The non-linear shape of the stress–strain curve (Fig. 2) indicated that the value of the tangent modulus varied with the strain level. Three clear regions of the curve were evident, describing a transition between a relatively flat toe, in which substantial strain (stretching) was required to increase stress, to a linear region where the tangent modulus remained approximately constant (Fig. 2A). These transitions indicate that swimbladder tissue is strain-stiffening because the tangent modulus was higher at higher strain values, excluding the failure response. The other notable behaviour was the progressive failure that occurred. For example, for sample 25, a clear drop in stress was observed at a strain of 1.4 (Fig. 2A). This drop corresponded to the formation and arresting of a tear in the tissue, after which the stress once again began to increase. Generally, the tear continues and propagates through the width of the tissue, indicating catastrophic failure. However, this was frequently not the case for the swimbladder tissue.

For part 2, in the longitudinal direction, the mean±s.d. maximum stress was 0.44±0.18 MPa while that in the circumferential direction was 0.42±0.18 MPa. The mean±s.d. tangent modulus was 0.68±0.34 and 0.37±0.18 MPa in the longitudinal and circumferential directions, respectively. Although no difference in strength was observed (W=48, P=0.91), the tangent modulus in the longitudinal direction was greater (stiffer) than in the circumferential direction (W=20, P<0.05). The observed changes in mechanical response in different directions suggest that the swimbladder wall is anisotropic; as a consequence, the data collected in the longitudinal and circumferential directions must be treated independently.

Swimbladder walls with lower tangent moduli tended to be the weaker (Fig. 3), and a strong linear correlation existed between the variables (longitudinal: r_s=0.88, P<0.01; circumferential: r_s=0.76, P<0.05).

Damage indicators

In comparing mechanical response with morphological indicators of damage in part 2, samples cut in the circumferential direction had higher wall thickness (t_{18}=4.81, P<0.01) and parasite load ($t_{10.9}$=2.54, P<0.05) than those cut in the longitudinal direction. There was no difference in LRI between the circumferential and longitudinal samples (t_{18}=1.45, P=0.16). Using the criteria in Table 1, the

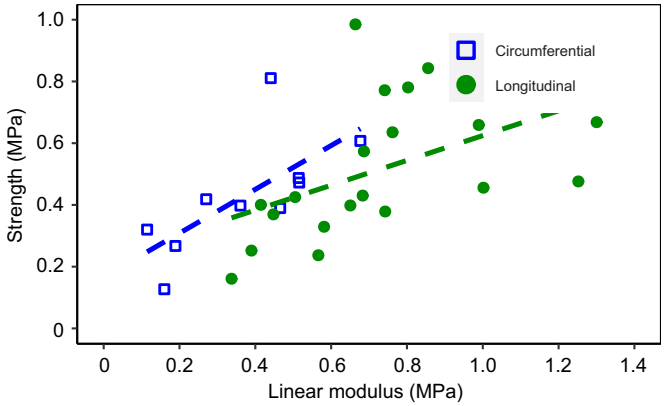

Fig. 3. Modulus in the linear region in the longitudinal and circumferential directions versus the maximum stress for the eel swimbladder wall. Circles, longitudinal direction (N=20); squares, circumferential direction (N=10).

Journal of Experimental Biology (2020) 223, jeb219808. doi:10.1242/jeb.219808

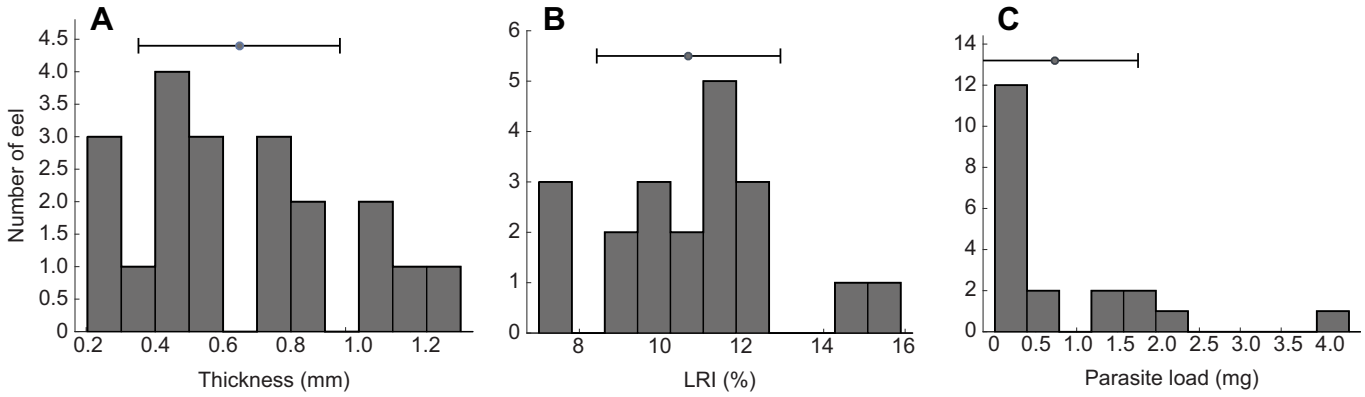

Fig. 4. Damage indicators used to identify eel population health status. Distribution of (A) thickness (mean±s.d.=0.67±0.34 mm); (B) length ratio index (LRI; 10.69±2.18%) and (C) parasite load (0.56±0.87 mg) of eel swimbladders. The horizontal bars indicate the mean±1 s.d. (*N*=20).

number of samples collected from relatively 'healthy' eel was determined; two were based on the thickness criteria, and 13 were based on LRI. The number of healthy eel increased to 19 when parasite load was considered, although this indicator only relates to current burden and provides no information on previous infection history. Nevertheless, the distribution of damage indictors (Fig. 4) suggests that the population of eel collected in this study had suffered minimal to moderate levels of infection.

Wall thickness was negatively correlated with maximum stress in both the circumferential and longitudinal directions (see Table S1). As thickness increased, the strength of the wall decreased with a correlation of −0.65 and −0.37 in the longitudinal and circumferential directions, respectively. In the longitudinal direction, the tangent modulus also showed a strong linear correlation with parasite load.

The relationship between wall thickness and rupture strength differed between the longitudinal and circumferential directions (Fig. 5). Examining the slopes of the curves, for the same increase in thickness the strength in the longitudinal direction tended to decrease by more than double. In the circumferential direction, there was greater scatter in the data as indicated by the lower correlation coefficient. Although the correlation coefficient identified between the parasite load and the longitudinal direction was high, there was considerable scatter (Fig. 6). The randomness was further confirmed when additional longitudinal data from the River Test were considered (see Fig. S2).

DISCUSSION

Utilising a novel approach, this study quantified changes in the mechanical properties of the European eel swimbladder wall in response to *A. crassus* infection. Results indicate that for moderate infection, the mechanical performance of the swimbladder is maintained by an increase in the thickness of the swimbladder wall, which occurs as part of a generalised immune response. This, however, leads to a trade-off: increasing thickness raises the pressure required for rupture, but decreases strength. Unlike for Japanese eel, which show immunocompetence to the parasite throughout its native environment (Knopf, 2006), here the tensile properties of the swimbladder material are changed from the uninfected condition, as a result of efforts to repair the damage. The findings of our study both support and explain the conclusions of earlier work conducted by Barry et al. (2014), in that more heavily infected swimbladders are less stiff (lower modulus) and would rupture at a higher pressure than uninfected swimbladders.

Assuming that the swimbladder is modelled as a thin-walled cylindrical pressure vessel, then the circumferential and longitudinal stress is a function of the wall thickness (t), the radius of the lumen (r) and the internal pressure (p):

$$\sigma_\theta = \frac{pr}{t}\ \sigma_z = \frac{pr}{2t}\ . \qquad (2)$$

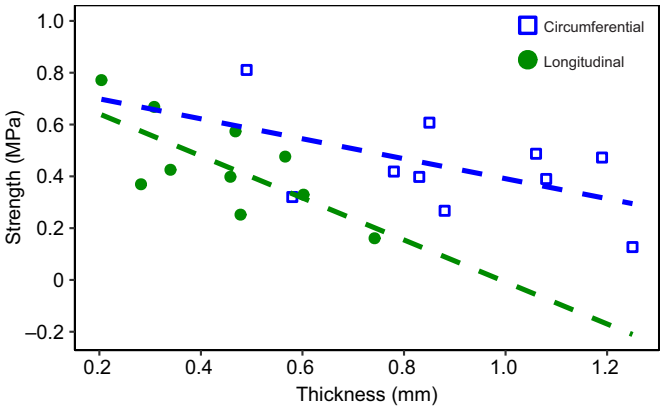

Fig. 5. Maximum stress in the longitudinal and circumferential directions versus the thickness. Circles, longitudinal direction (*N*=10); squares, circumferential direction (*N*=10). Regression line equations: $\sigma_{z,max}$=−0.811*t*+0.803 (longitudinal); $\sigma_{\theta,max}$=−0.385*t*+0.776 (circumferential).

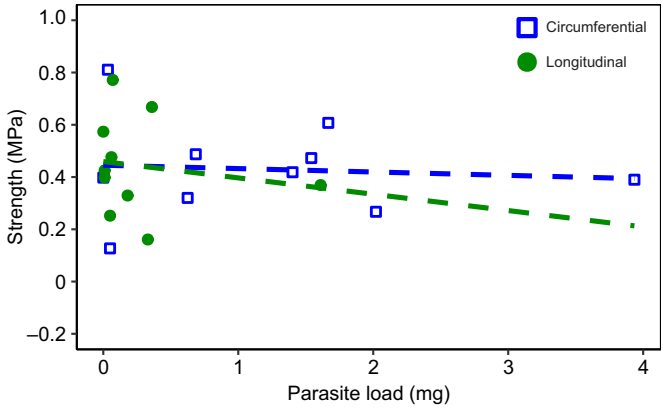

Fig. 6. Maximum stress in the longitudinal and circumferential direction versus the parasite load. Circles, longitudinal direction (*N*=10); squares, circumferential direction (*N*=10). Regression line equations: $\sigma_{z,max}$=−0.063*t*+0.459 (longitudinal); $\sigma_{\theta,max}$=−0.013*t*+0.445 (circumferential).

Using this model for the swimbladder, if the thickness is doubled, then for the same pressure the stress would be half for the thicker wall. If thick and thin swimbladders had the same strength, the thicker, repeatedly infected swimbladder would require more pressure to rupture. Wall strength decreases with increasing thickness, resulting in a trade-off for infected swimbladders: increasing the wall thickness is correlated with reductions in strength and simultaneously raises the pressure required for rupture.

The response of the swimbladder wall was also anisotropic, and therefore the mechanical response depends on the orientation of the sample. While the rupture stress was the same in both directions, samples taken along the longitudinal axis were nearly two times stiffer on average than those in the circumferential direction. Consequently, the relationship between the mechanical response and the damage indices was evaluated for each direction independently. By comparing the directional mechanical properties with pre-established damage indices, we determined that the wall thickness index, a proxy for severity of past infection, is the best indicator of rupture strength. Although the correlation was not significant for the circumferential samples, the relationship between thickness and rupture strength shows a very similar pattern to the longitudinal samples. This suggests that the other damage indices are not tracking mechanical damage, but more likely the morphological impact of the parasite.

Higher parasite mass correlated with a decrease in the maximum strength of the swimbladder in the longitudinal direction. This trend most likely reflected the small sample size of eel obtained from the River Stour. When additional data from the River Test were included, parasite load was not strongly correlated with rupture strength. It is possible that a high mass of parasites within the lumen prevents entry of the more mature juveniles (stage 4 in Kirk, 2003) resident in the swimbladder wall, as their migration is partially density mediated (Kirk, 2003). This leads to longer residence times in the swimbladder wall, resulting in it being constantly damaged with little chance to heal.

Molnár et al. (1993) described the histopathological changes in eel swimbladders infected by *A. crassus*. Infection is initially characterised by minor enlargement of the gas glands and dilatation of the blood vessels in the mucosa. Repeated infection by the blood-sucking nematodes creates epithelial lesions and leads to an inflammatory response, with serum accumulating between the fibres leading to thickening in the swimbladder wall. Chronic infection leads to narrowing of the lumen and the swimbladder wall becoming completely opaque. Combining the mechanical results of this study and previous histological work, we speculate that the wall hyperplasia occurs in response to stimulus initiated by the reduction in the strength and stiffness of the wall caused by the *A. crassus* infection. This change in geometry would, for moderate levels of infection, allow the swimbladder to maintain its mechanical performance. A similar response has been reported in blood vessels (Matsumoto and Hayashi, 1994), where hypertension leads to wall thickening, which reduces the stress in the circumferential direction. Further study is necessary to determine if and how the cells in the swimbladder wall respond to changes in mechanical stiffness.

Specimens in this study showed light to moderate swimbladder damage. Previous studies have found severe swimbladder degeneration only in the most mature eel, suggesting that damage accumulates from repeated infections throughout their lifetime. Higher body mass and total body length have been correlated with greater swimbladder damage (Costa-Dias et al., 2010; Kelly et al., 2000; Koops and Hartmann, 1989; Lefebvre et al., 2002, 2013; Palstra et al., 2007). Individual eel show a wide variation in foraging strategies, which in turn influences encounter rates and parasite burdens (Barry et al., 2017). The explanation given by Lefebvre et al. (2013) potentially explains our results: active foragers undergoing a large increase in size are more likely to get infected and caught by fishing gear, whereas eel in poor condition may be under-represented as they are less likely to be caught and may have reduced swimming and foraging capabilities due to infection.

While this study applies a more direct approach to understanding the impacts of repeated parasite infection on the mechanical response of the eel swimbladder, the approach does, however, have its limitations. The thickness ranges and corresponding damage levels are based on histology (Molnár et al., 1993). Routine histological processing can cause tissue distortion in samples. Shrinkage (Dobrin, 1996; Kerns et al., 2008) and expansion (Jeyakumar et al., 2015; Reagan et al., 2016; Reimer et al., 2005) have been reported for a variety of soft tissues with most estimates ranging between 10 and 25% dimensional change. The impact of the dehydration and embedding process is unknown for the eel swimbladder which means the thickness estimates applied here to fresh tissue are approximate.

Numerous biological indicators have been developed to assess European eel swimbladder degradation (Beregi et al., 1998; Lefebvre et al., 2011; Molnár et al., 1993). In this paper, the more complex swimbladder degenerative index (SDI) developed by Lefebvre et al. (2002) was not used. SDI is composed of three measurements: opacity, the presence of exudate and thickness. Lefebvre et al. (2011) critically evaluated the precision of LRI in comparison with SDI measurements and concluded that LRI was more reliable between investigator indicators. Improved performance was attributed to a reduced scope for subjectivity, increased precision of measurements, and better estimates of swimbladder volume reduction.

A purely mechanical approach to studying *A. crassus* damage does not directly capture the impact of any biochemical changes caused by the infection. A reduced efficiency of gas exchange due to an increased swimbladder wall thickness, which drastically reduces its permeability, has been reported (Kirk, 2003; Kobayashi et al., 1990). Structural changes increase the travel distance of acidic metabolites from epithelial cells to the blood vessels, leading to diffusional gas losses (Pelster, 2015; Würtz and Taraschewski, 2000). A swimbladder with impaired gas exchange may be highly debilitating, particularly under increased hydrostatic pressures (Alexander, 1966; Pelster, 2015). This could cause highly irregular swimming behaviour with the propensity to drastically drain energy reserves during the eel migration, which is a non-feeding life phase (Palstra et al., 2007; Sprengel and Lüchtenberg, 1991). It is also necessary, therefore, to consider the role of biochemical damage when quantifying the impact of *A. crassus*.

Although the European eel is considered to be a single population, one could reasonably expect some differences to arise between eels coming from two catchments. Part 1 of this study, however, investigated differences between modulus and maximum stress between longitudinal samples taken from two distinct river populations (River Stour and River Test, UK) and found this not to be the case. This result validated the approach taken in part 2 of this study, whereby owing to the conservation status of the eel, the number of swimbladders available for sampling was necessarily limited, originating from two separate regions of the UK. Numbers of eel successfully tested were further limited due to small-sized swimbladder (i.e. not adhering to template size), carcass purposing (i.e. tensile test versus histology), and testing issues (e.g. failure in the grips).

Future studies should be conducted to identify imaging modalities that can measure the thickness of the swimbladder wall in the European eel non-invasively. Previous studies have used radiography to estimate the volume of the swimbladder, and thereby infer the level of damage, based on size of the shadow in the X-ray images (Beregi et al., 1998; Frisch et al., 2016). However, the swimbladder wall is not visible in the X-ray images, limiting its ability to differentiate between the early stages of infection. Frisch et al. (2016) also used ultrasound imaging to visualise the swimbladder and while the images contain reverberation artefacts, the wall is clearly visible. A tool capable of estimating damage levels non-invasively would enable longitudinal tracking of eel populations and comprehensive estimates of infection levels in European catchments. Another possibility would be to combine ultrasound imaging with eel tagging (Righton et al., 2012, 2016) to collect data on the impact of swimbladder degeneration on the migration journey of the eel.

To conclude, thickening of the swimbladder wall results in a trade-off between increasing the pressure the swimbladder can withstand, but reducing the failure stress. Thus, it is likely that for mild infections the thickening of the swimbladder prevents catastrophic rupture of the swimbladder wall by compromising gas exchange efficiency (Kirk, 2003). Histology has shown that the thickening of the swimbladder wall is due to hyperplasia of the loose connective tissue layer (Molnár et al., 1993) and the mechanical results of this study have shown that thickening is linearly correlated with a reduction in the failure stress. Secondly, the mechanical response of the swimbladder wall in the European eel is anisotropic, likely to accommodate the different deformations experienced in the longitudinal and circumferential direction. The reduced stiffness in the circumferential axis would place lower energetic costs on expanding that direction, an action routinely used by an eel to modify its position in the water column. Although it is evident that parasitic infection is detrimental to the functionality of the swimbladder, it still remains unclear how severe the damage must be to impact migratory success. We suggest future attention should be directed towards utilising imaging technologies, such as micro computed tomography (μ-CT) to evaluate wholly intact swimbladder damage non-invasively (see Fig. S3 and Movie 1). This would allow for an in-depth assessment of swimbladder health in the current eel population and make further studies on the impact of swimbladder degeneration on migration possible.

Acknowledgements
The authors wish to thank Dr Toru Tsuzaki for his continued logistical support and Dr Orestis Katsamenis and Dr Susan Wilson (μ-VIS) for the CT scan imagery included in Figs S1, S3 and Movie 1.

Competing interests
The authors declare no competing or financial interests.

Author contributions
Conceptualization: P.S.K.; Methodology: H.A.L.C., N.F.M., G.E.G., F.M.D.; Formal analysis: H.A.L.C., F.M.D.; Investigation: H.A.L.C., N.F.M., G.E.G., F.M.D.; Writing - original draft: H.A.L.C., N.F.M., F.M.D.; Writing - review & editing: H.A.L.C., N.F.M., G.E.G., F.M.D., P.S.K.; Visualization: H.A.L.C., G.E.G., F.M.D.; Supervision: F.M.D., P.S.K.; Funding acquisition: F.M.D., P.S.K.

Funding
H.A.L.C., G.E.G. and N.F.M. were funded by the Training Grant for the EPSRC Centre for Doctoral Training in Sustainable Infrastructure Systems. F.M.D. was supported by a Leverhulme Trust Early Career Fellowship.

Data availability
All data accompanying this paper can be downloaded from the University of Southampton repository at: https://doi.org/10.5258/SOTON/D1184

Supplementary information
Supplementary information available online at
https://jeb.biologists.org/lookup/doi/10.1242/jeb.219808.supplemental

References
Aalto, E., Capoccioni, F., Terradez Mas, J., Schiavina, M., Leone, C., De Leo, G. and Ciccotti, E. (2016). Quantifying 60 years of declining European eel (*Anguilla anguilla* L., 1758) fishery yields in Mediterranean coastal lagoons. *ICES* **73**, 101-110. doi:10.1093/icesjms/fsv084

Aarestrup, K., Økland, F., Hansen, M. M., Righton, D., Gargan, P., Castonguay, M., Bernatch, L., Howey, P., Sparholt, H., Pedersen, M. I. et al. (2009). Oceanic spawning migration of the European eel (*Anguilla anguilla*). *Science* **325**, 1660. doi:10.1126/science.1178120

Acou, A., Laffaille, P., Legault, A. Feunteun, E. (2008). Migration pattern of silver eel (*Anguilla anguilla*, L.) in an obstructed river system. *Ecol. Freshw. Fish.* **17**, 432-442. doi:10.1111/j.1600-0633.2008.00295.x

Alexander, R. M. N. (1966). Physical aspects of swimbladder function. *Biol. Rev.* **41**, 141-176. doi:10.1111/j.1469-185X.1966.tb01542.x

Baltazar-Soares, M., Biastoch, A., Harrod, C., Hael, R., Marohn, L., Prigge, E., Evans, D., Bodles, K., Behrens, E., Böning, C. W. et al. (2014). Recruitment collapse and population structure of the European eel shaped by local ocean current dynamics. *Curr. Biol.* **24**, 104-108. doi:10.1016/j.cub.2013.11.031

Barry, J., McLeish, J., Dodd, J. A., Turnbull, J. F., Boylan, P. and Adams, C. E. (2014). Introduced parasite *Anguillicola crassus* infection significantly impedes swim bladder function in the European eel *Anguilla anguilla* (L.). *J. Fish. Dis.* **37**, 921-924. doi:10.1111/jfd.12215

Barry, J., Newton, M., Dodd, J. A., Evans, D., Newton, J. and Adams, C. E. (2017). The effect of foraging and ontogeny on the prevalence and intensity of the invasive parasite *Anguillicola crassus* in the European eel *Anguilla anguilla*. *J. Fish. Dis.* **40**, 1213-1222. doi:10.1111/jfd.12596

Beirão, B. V., Marciano, N. C. M., Dias, L. S., Falcão, R. C., Dias, E. W., Fabrino, D. L., Martinez, C. B., Silva, L. G. M., Walker, R., Brown, R. et al. (2015a). Barotrauma em peixes em usinas hidrelétricas: ferramentas para o estudo. *Boletim Sociedade Brasileira de Ictiologia.* **115**, 23-36.

Beirão, B., Silva, L. G. M. and Falcão, R. (2015b). New approach to evaluate barotrauma susceptibility in fish. American Fisheries Society 145th Annual Meeting, Portland, OR, USA.

Beregi, A., Molnár, K., Békési, L. and Székely, C. (1998). Radiodiagnostic method for studying swimbladder inflammation caused by *Anguillicola crassus* (Nematoda: Dracunculoidea). *Dis. Aquat. Organ.* **34**, 155-160. doi:10.3354/dao034155

Bornarel, V., Lambert, P., Briand, C., Antunes, C., Belpaire, C., Ciccotti, E., Diaz, E., Diserud, O., Doherty, D., Domingos, I. et al. (2018). Modelling the recruitment of European eel (*Anguilla anguilla*) throughout its European range. *ICES* **75**, 541-552. doi:10.1093/icesjms/fsx180

Brown, R. S., Colotelo, A. H., Pflugrath, B. D., Boys, C. A., Baumgartner, L. J., Deng, Z. D., Silva, L. G. M., Brauner, C. J., Mallen-Cooper, M., Phonekhampeng, O. et al. (2014). Understanding barotrauma in fish passing hydro structures: a global strategy for sustainable development of water resources. *Fisheries* **39**, 108-122. doi:10.1080/03632415.2014.883570

Costa-Dias, S., Dias, E., Lobón-Cerviá, J., Antunes, C. and Coimra, J. (2010). Infection by *Anguillicoloides crassus* in a riverine stock of European eel, *Anguilla anguilla*. *Fisheries Manag. Ecol.* **17**, 485-492. doi:10.1111/j.1365-2400.2010.00746.x

De Charleroy, D., Grisez, L., Thomas, K., Belpaire, C. and Ollevier, F. (1990). The life cycle of *Anguillicola crassus*. *Dis. Aquat. Organ.* **8**, 77-84. doi:10.3354/dao008077

Dekker, W. (2003). Did lack of spawners cause the collapse of the European eel, *Anguilla anguilla*? *Fish. Manag. Ecol.* **10**, 365-376. doi:10.1111/j.1365-2400.2003.00352.x

Dobrin, P. B. (1996). Effect of histologic preparation on the cross-sectional area of arterial rings. *J. Surg. Res.* **61**, 413-415. doi:10.1006/jsre.1996.0138

Dorn, E. (1961). Über den Feinbauder Schwimmblase von *Anguilla vulgaris* L. Licht- und Elektronen mikroskopische Untersuchungen. *Z. Zellforsch.* **55**, 849-912. doi:10.1007/BF00381654

Frisch, K., Davie, A., Schwarz, T. and Turnbull, J. F. (2016). Comparative imaging of European eels (*Anguilla anguilla*) for the evaluation of swimbladder nematode (*Anguillicoloides crassus*) infestation. *J. Fish. Dis.* **39**, 635-647. doi:10.1111/jfd.12383

ICES (2017). *Report of the Joint EIFAAC/ICES/GFCM Working Group on Eels*. International Council for the Exploration of the Sea, Copenhagen: Denmark.

Jacoby, D. and Gollock, M. (2014). *Anguilla anguilla*. The IUCN Red List of Threatened Species 2014. https://dx.doi.org/10.2305/IUCN.UK.2020-2.RLTS.T60344A152845178.en

Jacoby, D. M. P., Casselman, J. M., Crook, V., DeLucia, M.-B., Ahn, H., Kaifu, K., Kurwie, T., Sasal, P., Silfvergrip, A. M. C., Smith, K. G. et al. (2015). Synergistic patterns of threat and the challenges facing global anguillid eel conservation. *Glob. Ecol. Conserv.* **4**, 321-333. doi:10.1016/j.gecco.2015.07.009

Jeyakumar, S., Smith, A. N., Schleis, S. E., Cattley, R. C., Tillson, D. M. and Henderson, R. A. (2015). Effect of histologic processing on dimensions of skin samples obtained from cat cadavers. *Am. J. Vet. Res.* **76**, 939-945. doi:10.2460/ajvr.76.11.939

Kelly, C. E., Kennedy, C. R. and Brown, J. A. (2000). Physiological status of wild European eels (*Anguilla anguilla)* infected with the parasitic nematode, *Anguillicola crassus*. *Parasitology*. **120**, 195-202. doi:10.1017/S0031182099005314

Kennedy, C. R. (1993). Introductions, spread and colonization of new localities by fish helminth and crustacean parasites in the British Isles: a perspective and appraisal. *J. Fish. Biol.* **43**, 287-301. doi:10.1111/j.1095-8649.1993.tb00429.x

Kerns, M. J. J., Darst, M. A., Olsen, T. G., Fenster, M., Hall, P. and Grevey, S. (2008). Shrinkage of cutaneous specimens: formalin or other factors involved? *J. Cutan. Pathol.* **35**, 1093-1096. doi:10.1111/j.1600-0560.2007.00943.x

Kirk, R. S. (2003). The impact of *Anguillicola crassus* on European eels. *Fisheries Manag. Ecol.* **10**, 385-394. doi:10.1111/j.1365-2400.2003.00355.x

Knopf, K. (2006). The swimbladder nematode *Anguillicola crassus* in the European eel *Anguilla anguilla* and the Japanese eel *Anguilla japonica*: differences in susceptibility and immunity between a recently colonized host and the original host. *J. Helminthol.* **80**, 129-136. doi:10.1079/JOH2006353

Kobayashi, H., Pelster, B. and Scheid, P. (1990). CO_2 back-diffusion in the rete aids O_2 secretion in the swimbladder of the eel. *Respir. Physiol.* **79**, 231-242. doi:10.1016/0034-5687(90)90129-M

Koops, H. and Hartmann, F. (1989). Anguillicola-infestations in Germany and in German eel imports. *J. Appl. Ichthyol.* **5**, 41-45. doi:10.1111/j.1439-0426.1989.tb00568.x

Lefebvre, F., Contournet, P. and Crivelli, A. J. (2002). The health state of the eel swimbladder as a measure of parasite pressure by *Anguillicola crassus*. *Parasitology* **124**, 457-463. doi:10.1017/S0031182001001378

Lefebvre, F., Fazio, G., Mounaix, B. and Crivelli, A. J. (2013). Is the continental life of the European eel *Anguilla anguilla* affected by the parasitic invader *Anguillicoloides crassus*? *Proc. R. Soc. B* **280**, 20122916. doi:10.1098/rspb.2012.2916

Lefebvre, F., Fazio, G., Palstra, A. P., Székely, C. and Crivelli, A. J. (2011). An evaluation of indices of gross pathology associated with the nematode *Anguillicoloides crassus* in eels. *J. Fish. Dis.* **34**, 31-45. doi:10.1111/j.1365-2761.2010.01207.x

Lefebvre, F., Wielgoss, S., Nagasawa, K. and Moravec, F. (2012). On the origin of *Anguillicoloides crassus*, the invasive nematode of anguillid eels. *Aquat. Invasions.* **7**, 443-453. doi:10.3391/ai.2012.7.4.001

Matsumoto, T. and Hayashi, K. (1994). Mechanical and dimensional adaptation of rat aorta to hypertension. *J. Biomech. Eng.* **116**, 278-283. doi:10.1115/1.2895731

Miller, M. J., Feunteun, E. and Tsukamoto, K. (2015). Did a 'perfect storm' of oceanic changes and continental anthropogenic impacts cause northern hemisphere anguillid recruitment reductions? *ICES* **73**, 43-56. doi:10.1093/icesjms/fsv063

Molnár, K., Baska, F., Csaba, G., Glávits, R. and Székely, C. (1993). Pathological and histopathological studies of the swimbladder of eels *Anguilla anguilla* infected by *Anguillicola crassus* (Nematoda : Dracunculoidea). *Dis. Aquat. Organ.* **15**, 41-50. doi:10.3354/dao015041

Molnár, K., Szakolczai, J. and Vetési, F. (1995). Histological changes in the swimbladder wall of eels due to abnormal location of adults and 2nd stage larvae of *Anguillicola crassus*. *Acta. Vet. Hung.* **43**, 125-137.

Newbold, L. R., Hockley, F. A., Williams, C. F., Cable, J., Reading, A. J., Auchterlonie, N. and Kemp, P. S. (2015). Relationship between European eel *Anguilla anguilla* infection with non-native parasites and swimming behaviour on encountering accelerating flow. *J. Fish. Biol.* **86**, 1519-1533. doi:10.1111/jfb.12659

Nimeth, K., Zwerger, P., Würtz, J., Salvenmoser, W. and Pelster, B. (2000). Infection of the glass-eel swimbladder with the nematode *Anguillicola crassus*. *Parasitology* **121**, 75-83. doi:10.1017/S003118209900606X

Palstra, A. P., Heppener, D. F. M., van Ginneken, V. J. T., Székely, C. and van den Thillart, G. E. E. J. M. (2007). Swimming performance of silver eels is severely impaired by the swim-bladder parasite *Anguillicola crassus*. *J. Exp. Mar. Biol. Ecol.* **352**, 244-256. doi:10.1016/j.jembe.2007.08.003

Pelster, B. (2015). Swimbladder function and the spawning migration of the European eel *Anguilla anguilla*. *Front. Physiol.* **6**, 1-10. doi:10.3389/fphys.2014.00486

Reagan, J. K., Selmic, L. E., Garrett, L. D. and Singh, K. (2016). Evaluation of the effects of anatomic location, histologic processing, and sample size on shrinkage of skin samples obtained from canine cadavers. *Am. J. Vet. Res.* **77**, 1036-1044. doi:10.2460/ajvr.77.9.1036

Reimer, S. B., Séguin, B., DeCock, H. E., Walsh, P. J. and Kass, P. H. (2005). Evaluation of the effect of routine histologic processing on the size of skin samples obtained from dogs. *Am. J. Vet. Res.* **66**, 500-505. doi:10.2460/ajvr.2005.66.500

Righton, D., Aarestrup, K., Jellyman, D., Sébert, P., van den Thillart, G. and Tsukamoto, K. (2012). The *Anguilla* spp. migration problem: 40 million years of evolution and two millennia of speculation. *J. Fish. Biol.* **81**, 365-386. doi:10.1111/j.1095-8649.2012.03373.x

Righton, D., Westerberg, H., Feunteun, E., Økland, F., Gargan, P., Amilhat, E., Metcalfe, J., Lobon-Cervia, J., Sjöberg, N., Simon, J. et al. (2016). Empirical observations of the spawning migration of European eels: the long and dangerous road to the Sargasso Sea. *Sci. Adv.* **2**, e1501694. doi:10.1126/sciadv.1501694

Russell, W. M. S. and Burch, R. L. (1959). *The Principles of Humane Experimental Technique*. Wheathampstead, UK: Universities Federation for Animal Welfare.

Sébert, M.-E., Amérand, A., Vettier, A., Weltzien, F.-A., Pasqualini, C., Sébert, P. and Dufour, S. (2007). Effects of high hydrostatic pressure on the pituitary–gonad axis in the European eel, *Anguilla anguilla* (L.). *Gen. Comp. Endocrinol.* **153**, 289-298. doi:10.1016/j.ygcen.2007.01.009

Sjöberg, N. B., Petersson, E., Wickström, H. and Hansson, S. (2009). Effects of the swimbladder parasite *Anguillicola crassus* on the migration of European silver eels *Anguilla anguilla* in the Baltic Sea. *J. Fish. Biol.* **74**, 2158-2170. doi:10.1111/j.1095-8649.2009.02296.x

Sokolowski, M. S. and Dove, A. D. M. (2006). Histopathological examination of wild American eels infected with *Anguillicola crassus*. *J. Aquat. Anim. Health.* **18**, 257-262. doi:10.1577/H06-009.1

Sprengel, G. and Lüchtenberg, H. (1991). Infection by endoparasites reduces maximum swimming speed of European smelt *Osmerus eperlanus* and European eel *Anguilla anguilla*. *Dis. Aquat. Organ.* **11**, 31-35. doi:10.3354/dao011031

Székely, C., Palstra, A., Molnár, K. and van den Thillart, G. (2009). Impact of the Swim-Bladder Parasite on the Health and Performance of European Eels. In *Spawning Migration of the European Eel* (ed. G. van den Thillart, S. Dufour and J.C. Rankin), pp. 201-226. Dordrecht: Springer, Netherlands.

van den Thillart, G., van Ginneken, V., Körner, F., Heijmans, R., van der Linden, R. and Gluvers, A. (2004). Endurance swimming of European eel. *J. Fish. Biol.* **65**, 312-318. doi:10.1111/j.0022-1112.2004.00447.x

Wielgoss, S., Taraschewski, H., Meyer, A. and Wirth, T. (2008). Population structure of the parasitic nematode *Anguillicola crassus*, an invader of declining North Atlantic eel stocks. *Mol. Ecol.* **17**, 3478-3495. doi:10.1111/j.1365-294X.2008.03855.x

Würtz, J. and Taraschewski, H. (2000). Histopathological changes in the swimbladder wall of the European eel *Anguilla anguilla* due to infections with *Anguillicola crassus*. *Dis. Aquat. Organ.* **39**, 121-134. doi:10.3354/dao039121